

# Phosphorylation of histone H3 at Thr3 is part of a combinatorial pattern that marks and configures mitotic chromatin

Yolanda Markaki<sup>1</sup>, Anastasia Christogianni<sup>1</sup>, Anastasia S. Politou<sup>2</sup> and Spyros D. Georgatos<sup>1,\*</sup>

<sup>1</sup>Laboratory of Biology and <sup>2</sup>Laboratory of Biological Chemistry, Stem Cell and Chromatin Group, The University of Ioannina School of Medicine and The Biomedical Institute of Ioannina (BRI/FORTH), Dourouti, 45 110 Ioannina, Greece

\*Author for correspondence (sgeorgat@cc.uoi.gr)

Accepted 5 May 2009

Journal of Cell Science 122, 2809-2819 Published by The Company of Biologists 2009  
doi:10.1242/jcs.043810

## Summary

We have previously shown that histone H3 is transiently phosphorylated at Thr3 during mitosis. Extending these studies, we now report that phosphorylated Thr3 is always in *cis* to trimethylated Lys4 and dimethylated Arg8, forming a new type of combinatorial modification, which we have termed PMM. PMM-marked chromatin emerges at multiple, peripheral sites of the prophase nucleus, then forms distinct clusters at the centric regions of metaphase chromosomes, and finally spreads (as it wanes) to the distal areas of segregating chromatids. The characteristic prophase pattern can be reproduced by expressing ectopically the kinase haspin at interphase, suggesting that the formation of the PMM signature does not require a pre-existing mitotic environment. On the other hand,

the ‘dissolution’ and displacement of PMM clusters from a centric to distal position can be induced by partial dephosphorylation or chromosome unravelling, indicating that these changes reflect the regulated grouping and scrambling of PMM subdomains during cell division. Formation of PMM is prevented by haspin knockdown and leads to delayed exit from mitosis. However, PMM-negative cells do not exhibit major chromosomal defects, suggesting that the local structures formed by PMM chromatin may serve as a ‘licensing system’ that allows quick clearance through the metaphase-anaphase checkpoint.

Key words: Chromatin, Histones, Phosphorylation

## Introduction

It is becoming increasingly clearer that histone modifications occur in patterns (Jiang et al., 2007; Taverna et al., 2006; Phanstiel et al., 2008; Trojer and Reinberg, 2008). Transcriptionally active loci and euchromatic territories are known to contain histone H3 trimethylated at lysine-4 (H3K4me<sub>3</sub>; from this point on, histone modifications are indicated by the initials of each histone, followed by the specific residue that is modified and the number of methyl, phospho or acetyl groups attached) as well as H3K4me<sub>2</sub>, H3K36me<sub>3</sub> and H4ac. Regions of transcriptionally silent, constitutive heterochromatin are enriched in H3K9me<sub>3</sub>, H3K27me<sub>1</sub> and H4K20me<sub>3</sub>; and facultative heterochromatin contains H3K9me<sub>2</sub>, H3K27me<sub>3</sub> and H4K20me<sub>1,3</sub>.

For some reason, simple indexing rules that apply well to histone methylation and acetylation do not seem to describe histone phosphorylation, a modification that occurs in seemingly disparate situations. For instance, phosphorylation of histone H3 is induced when interphase cells are stimulated by growth factors and enter a transcriptionally hyperactive state, but the same happens during mitosis when chromatin compacts and transcriptional activity ceases (Cheung et al., 2000). Moreover, phosphorylation of histone H2A.X (γ-H2A.X) occurs ‘generically’ after DNA damage (Rogakou et al., 1998), but the same is also observed under physiologically unique circumstances, e.g. stimulation of the inotropic glutamate receptors in cortical neurons (Crowe et al., 2006).

By and large, the most extensively phosphorylated core histone is H3 (Shoemaker and Chackley, 1978). Typical modifications in this histone form are phosphorylated H3S10 (H3S10phos), H3S28phos (Hendzel et al., 1997; De Souza et al., 2000; Hake et

al., 2005), H3T11phos (Preuss et al., 2003) and H3T3phos (Polioudaki et al., 2004; Dai et al., 2005), all located in the N-terminal tail of the molecule. H3S10phos, in combination to H3K9me<sub>3</sub>, are believed to provide a ‘binary switch’, which determines recruitment or eviction of HP1 proteins from pericentromeric heterochromatin (Fischle et al., 2005). However, H3T3phos, a reversible modification that occurs during mitosis and is catalyzed by the kinase haspin (Dai et al., 2005), has been implicated in sister chromatid cohesion (Dai et al., 2006).

Despite significant advances in the field of histone phosphorylation, key mechanistic questions remain unanswered. For example, it is not clear whether the site-specific phosphorylation of a particular serine or threonine residue represents a ‘point-signal’, or a part of a more complex read-out that includes adjacent modifications in *cis* (in the same histone molecule) and in *trans* (in different histone tails). Furthermore, it is not known whether serine/threonine phosphorylation creates new binding sites for chromatin-associated proteins (as presumably does lysine methylation), or whether it affects chromatin folding directly. The current study represents an effort to tackle these questions, using a multifaceted biochemical and morphological approach.

## Results

Histone modifications associated with H3T3phos

As mentioned above, H3T3phos occurs specifically in mitosis. To examine whether this mark is associated with other histone modifications, we developed a suitable fractionation scheme for isolating H3T3phos-containing nucleosomes from mitotic cells. In

brief, chromosomes prepared from nocodazole-arrested cells were subjected to controlled sonication, digested with nuclease and extracted with moderate (0.3 M) salt. Chromatin fragments released in a 100,000 *g* supernatant were then collected and fractionated in sucrose density gradients.

As shown in Fig. 1A,B, the high-speed chromosome extract contained predominantly mono-nucleosomes and, to a much lesser

extent, higher oligomeric species. Chromatin fragments bearing H3T3phos were isolated from this material using an affinity-purified antibody to H3T3phos (aP3). The fraction precipitated by aP3 corresponded to about 5% of the input nucleosomes (Fig. 1C), indicating that H3T3phos is restricted to a specific subclass of particles. Consistent with this interpretation, proteins associated with bulk euchromatin (e.g. SNF2), centromeric chromatin (e.g. CENP-A), pericentromeric heterochromatin (e.g. HP1 $\alpha$ ) and major mitotic kinases (such as cdc2 and Aurora B) were not detected in the aP3 immunoprecipitate (Fig. 1D). Furthermore, nucleosomal DNA coprecipitating with H3T3phos-containing particles corresponded to fragments of ~150 bp, i.e. mononucleosomes, whereas the DNA that was left behind in the immunoprecipitation supernatant also contained larger nucleosomal arrays (Fig. 1E).

H3T3phos-containing nucleosomes possessed a unique set of histone H3 modifications (Fig. 1F). These included: (1) H3S10phos and H3K4me<sub>2</sub>, which have been previously identified in the inner centromeric zone of metaphase chromosomes (Blower and Karpen, 2001; Sullivan and Karpen, 2004); (2) H3K9me<sub>3</sub>, a mark related to pericentromeric heterochromatin; and (3) H3K4me<sub>3</sub> in combination with H3K27me<sub>3</sub>, a rare bivalent modification that has been detected so far only in undifferentiated stem cells (Bernstein et al., 2006).

To examine more systematically the nature of modifications that co-exist with H3T3phos, immuno-isolated chromatin fractions were run on SDS gels and the H3 band was cut out and processed for mass spectrometry (MALDI-TOF). As seen in Table 1, all the site-specific modifications that were previously detected by western blotting could also be identified by this approach. In addition to these, we also noticed that in three out of three independent experiments the spectra contained a characteristic peak at 854.41 Da, matching (in mass) a peptide that extends from Thr3 to Arg8 plus an additional 150 Daltons. This mass difference was suggestive of a complex modification pattern corresponding either to one phosphate and five methyl groups, or to one phosphate, one acetyl and two methyl groups.

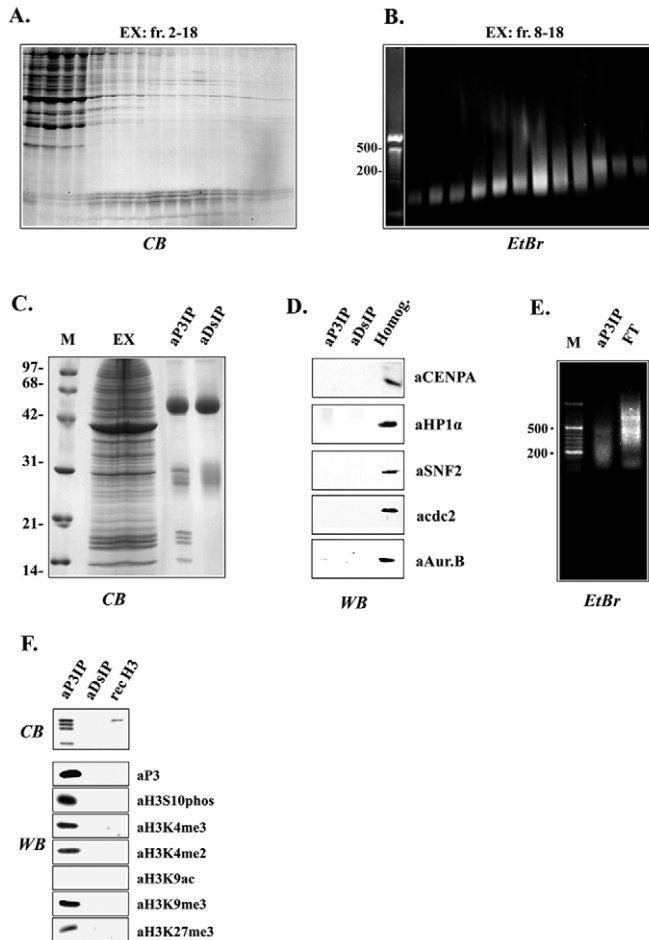


**Fig. 1.** Isolation and characterization of H3T3phos -marked chromatin. (A,B) Profiles of a typical chromosome extract (EX) fractionated in a 10-40% sucrose gradient and analyzed for protein and DNA. A Coomassie-blue-stained polyacrylamide gel of the indicated fractions is shown on the left (CB) and an agarose gel stained with ethidium bromide is depicted on the right (EtBr). DNA markers of 200 and 500 bp are indicated. (C) Chromatin immunoprecipitation using the aP3 antibody. A polyacrylamide gel (CB) containing 10% of the input (EX) and 100% of the proteins precipitated by anti-P3 (aP3IP) or control, anti-desmin antibodies (aDsIP) is shown here. Molecular size markers with the indicated values (in kDa) are on the left. (D,E) Non-histone components associated with H3T3phos. Western blots (WB) of a total mitotic homogenate (Homog.), aP3IP and aDsIP are shown in D. The blots were probed with aCENP-A, aHP1 $\alpha$ , aSNF2, acdc2 and aAurora B antibodies, as indicated. Profiles of DNA in the aP3IP fraction, or remaining in the immunoprecipitation supernatant (FT), are shown in E after ethidium bromide staining of the corresponding agarose gel. DNA markers of 200 and 500 bp are highlighted. (F) Detection of histone H3 modifications in the material precipitated by anti-P3 (aP3IP; see above). The aDsIP control and a sample of recombinant histone H3 (rec.H3) are also included for comparative purposes. The box on top shows the core histone region on a Coomassie-blue-stained gel (CB), whereas the lower panels depict the relevant area of the corresponding western blots (WB) using aP3, aH3S10phos, aH3K4me<sub>3</sub>, aH3K4me<sub>2</sub>, aH3K9ac, aH3K9me<sub>3</sub> and aH3K27me<sub>3</sub> antibodies.

**Table 1. MALDI-TOF data analysis of aP3-precipitated histone H3**

Peak (Da)	Residues	$\Delta M$ (Da)	Modification
854.41	3-8	150	5 $\times$ me(ac+2 $\times$ me)+P
901.52	9-17	0	nm
999.52	9-17	98	7 $\times$ me(2 $\times$ ac+me)
1061.52	9-17	160	2 $\times$ P
1065.52	9-17	164	2 $\times$ ac(6 $\times$ me)+P
1845.93	3-8 and 9-17	240	3 $\times$ P
986.61	18-26	0	nm
1433.83	27-40	0	nm
1461.83	27-40	28	2 $\times$ me
1475.83	27-40	42	3 $\times$ me(ac)
1489.83	27-40	56	4 $\times$ me(me+ac)
1635.83	27-40	202	3 $\times$ me(ac)+2P
1060.60	41-49	28	2 $\times$ me
1250.71	54-63	0	nm
788.48	64-69	0	nm
1335.69	73-83	0	nm
1384.80	117-128	0	nm
1478.80	117-128	94	me+P

The peaks detected and the differences in mass ( $\Delta M$ ) with respect to unmodified stretches (nm) are shown. P, phosphorylation; me, methylation; ac, acetylation at different residues, inferred from the corresponding  $\Delta M$ . For more details see text.

The single phosphate group could be easily assigned to Thr3, because the H3 sample was obtained by immunoprecipitation with an H3T3phos-specific antibody. Alternatively, three methyl groups could be ascribed to H3K4me<sub>3</sub> (and not H3K4ac), because this mark was readily detectable by western blotting. That, however, left two more methyl groups unaccounted for, the presence of which could only be explained if Arg8 were dimethylated. Making this assumption, we hypothesized that the H3 peptide extending from Thr3 to Arg8 contained three distinctly modified residues: H3T3phos, H3K4me<sub>3</sub> and H3R8me<sub>2</sub>. For brevity, we termed this combinatorial mark 'PMM', from the initials of the corresponding modifications.

#### Identification of the PMM mark in vivo

To confirm the MALDI-TOF results by an independent method, we immunized rabbits with a synthetic H3 peptide (a 15mer) containing H3T3phos, H3K4me<sub>3</sub> and H3R8me<sub>2</sub> (PMM) and used the resulting immune sera to examine whether the PMM mark exists in vivo. Consistent with our previous observations, antibodies affinity-purified using as a matrix the PMM peptide (aPMM) stained exclusively mitotic figures (Fig. 2A). Furthermore, in western blots, aPMM gave a positive reaction with the histone H3 fraction precipitated by aP3, whereas aP3 reacted equally well with histone H3 precipitated by aPMM (Fig. 2B). Finally, all H3 modifications detected in the aP3 immunisolate, i.e. H3S10phos, H3K4me<sub>2</sub>, H3K4me<sub>3</sub>, H3K9me<sub>3</sub> and

H3K27me<sub>3</sub>, but not H3K9ac, were also identified in the fraction of H3 precipitated by aPMM (Fig. 2C; compare with Fig. 1E). Therefore, the aPMM antibody appeared to recognize the same histone H3 sub-species as aP3.

In conventional ELISA assays (Fig. 2D), aPMM bound strongly to the immunogenic PMM peptide that contained the full set of modifications, but did not react with peptides bearing single modifications (H3T3phos, H3K4me<sub>3</sub>, H3R8me<sub>2</sub>). With peptides that carried two modifications, a modest reaction was observed with H3T3phos-H3K4me<sub>3</sub> and a weak (but measurable) reaction was seen with a peptide bearing H3K4me<sub>3</sub>-H3R8me<sub>2</sub>. However, aPMM did not react at all with the peptide possessing H3T3phos-H3R8me<sub>2</sub>. These results suggested that aPMM contains three serologically distinct specificities: (1) high-affinity antibodies against the full combinatorial epitope PMM; (2) antibodies with a modest affinity for H3T3phos-H3K4me<sub>3</sub>; and (3) antibodies with low affinity for the H3K4me<sub>3</sub>-R8me<sub>2</sub> combination.

When the ELISA assays were repeated in a competitive mode (Fig. 2E), only the PMM peptide, and to a lesser extent the H3T3phos-H3K4me<sub>3</sub> peptide, were able to compete, whereas all other peptides had a negligible effect. In addition, when we probed mitotic cells with the affinity-purified aPMM antibody, the PMM peptide, which contained the full set of marks, completely inhibited chromosome staining, whereas the H3T3phos-H3K4me<sub>3</sub> peptide had a less dramatic effect. None of the other peptides, including

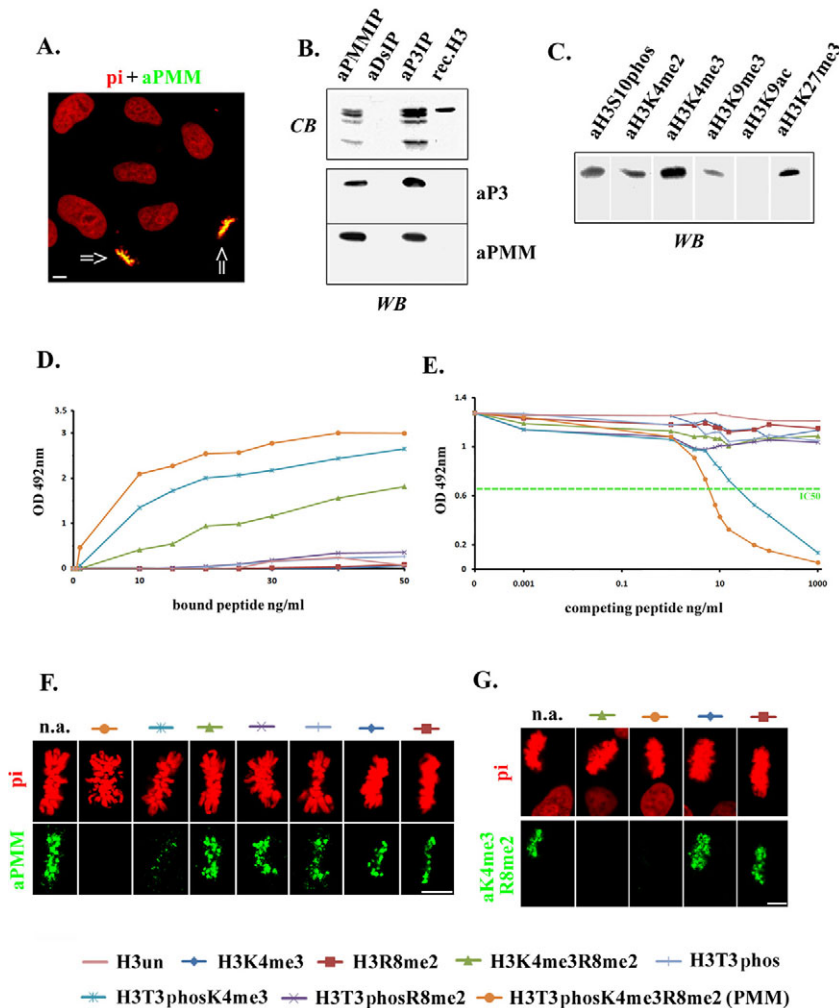


**Fig. 2.** Characterization of aPMM antibodies. (A) Staining of an unsynchronous culture with aPMM and propidium iodide (pi). Note that only mitotic figures are labeled (arrows). Scale bar: 5  $\mu$ m. (B) Comparative biochemical analysis of material precipitated by anti-P3 (aP3IP), anti-PMM (aPMMIP) and control antibodies (aDsIP) from the same mitotic extract. Recombinant histone H3 (rec.H3) is included as a negative control. The upper panel corresponds to a Coomassie-blue-stained gel (CB), whereas the lower panel shows blots with aP3 and aPMM antibodies. (C) Detection of histone H3 modifications in the material precipitated by aPMM. The panel depicts the relevant area of the corresponding western blots (WB) using antibodies against H3S10phos, H3K4me<sub>2</sub>, H3K4me<sub>3</sub>, H3K9me<sub>3</sub>, H3K9ac and H3K27me<sub>3</sub>. (D) Reactivity of aPMM with different H3 peptides, as assessed by conventional ELISA assays. See key at bottom of figure. (E) The same assay as shown in D, executed in a competitive mode. Broken line indicates 50% displacement. For further details see text. (F,G) Staining of metaphase cells by antibodies affinity-purified against a H3T3phos-K4me<sub>3</sub>-R8me<sub>2</sub> (PMM)-matrix in the presence and absence of different H3 peptides. The top series shows the pi channel and the bottom series shows antibody staining. Scale bar: 5  $\mu$ m. n.a., indicates no additions; in all other samples the peptides were included at 500 ng/ml.

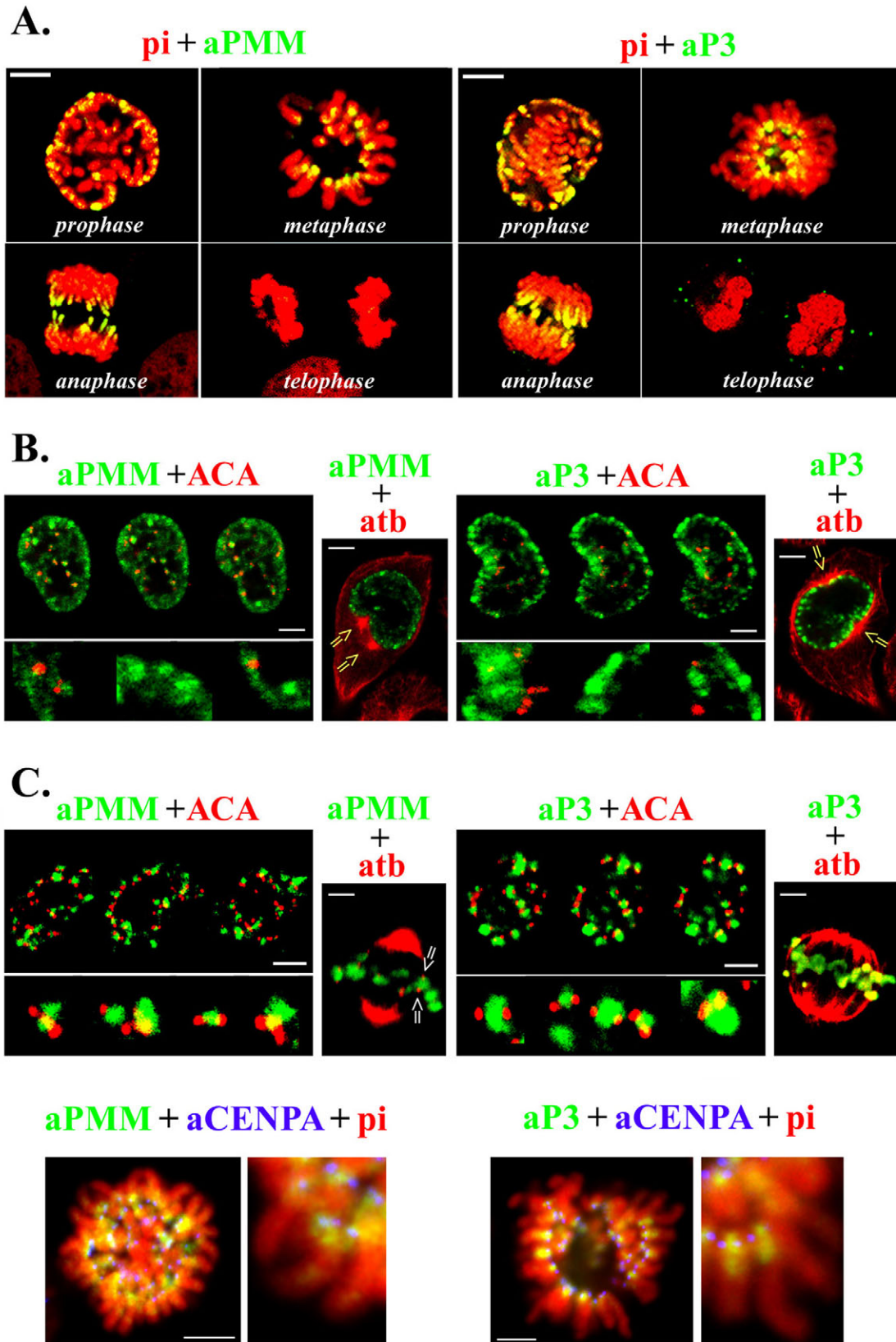


**Fig. 3.** Spatio-temporal patterns of PMM and H3T3phos during mitosis. (A) Profiles of mitotic cells stained with aPMM or aP3 plus propidium iodide (pi). Selected optical sections corresponding to the different phases of cell division are shown. (B,C) Localization of PMM and H3T3phos in relation to CENP antigens and microtubules during prophase (B) and metaphase (C). Co-staining with anti-tubulin (atb) and ACA or aCENP-A antibodies is shown. Yellow arrows in B indicate microtubule asters developing from centrosomes, whereas white arrows in C indicate sites of microtubule attachment at kinetochores. For more clarity, profiles of some doubly decorated regions are depicted in the galleries shown directly below or next to the images at higher contrast and magnification. Scale bars: 5  $\mu$ m.

H3K4me<sub>3</sub>-R8me<sub>2</sub>, affected either the intensity or the pattern of the immunofluorescence signal (Fig. 2F).

In combination, the data obtained in the two types of competitive assay (Fig. 2E,F), although consistent with our initial assumptions, were somewhat contradictory to what was seen in conventional ELISA assays (Fig. 2D) and did not clarify whether the double H3K4me<sub>3</sub>-H3R8me<sub>2</sub> mark existed *in vivo* (because this peptide did not compete). To address this problem, instead of using the PMM peptide as an immuno-affinity matrix, we passed the original immune sera through a H3K4me<sub>3</sub>-H3R8me<sub>2</sub> column and tried to isolate the putative aH3K4me<sub>3</sub>-H3R8me<sub>2</sub> antibody in a more concentrated and purified form. As shown in Fig. 2G, the immunoglobulin eluted from this column readily decorated mitotic chromosomes similarly to affinity-purified aPMM. Furthermore, chromosome staining was completely abolished by the H3K4me<sub>3</sub>-H3R8me<sub>2</sub> and the PMM peptides that contained the corresponding modifications, while singly modified peptides, such as H3K4me<sub>3</sub> and H3R8me<sub>2</sub>, did not affect at all the intensity or the quality of the fluorescence signal. From these data we concluded that the H3K4me<sub>3</sub>-H3R8me<sub>2</sub> sub-epitope is an integral part of the PMM signature and that this signature exists *in vivo*.

#### Patterns of PMM-marked chromatin in intact mitotic cells

Having established that the PMM mark exists *in vivo*, we performed a comprehensive confocal microscopy study to compare its spatio-temporal pattern with that of H3T3phos. As shown in Fig. 3, the staining patterns of the two modifications were identical. Specific fluorescence could be discerned first in prophase. In this stage of mitosis, PMM and H3T3phos were detected primarily in chromosome areas facing the nuclear envelope, yielding an imperfect 'rim' in equatorial sections (Fig. 3A, prophase). The sites containing PMM and H3T3phos were not spatially associated with the centromeres, as assessed by autoantibodies (ACA) to the centromeric passenger proteins CENP-B and CENP-C and the centromere-specific H3 variant CENP-A. Furthermore, PMM- and H3T3phos-marked chromatin was not particularly concentrated in the 'sinuses' of the nuclear envelope, which develop during prophase and accommodate the growing aster microtubules (Fig. 3B) (Georgatos et al., 1997).

The PMM and H3T3phos pattern changed dramatically at metaphase, when domains of modified chromatin were seen to focus on the centromere (Fig. 3A, metaphase). The close spatial relationship between PMM- and H3T3phos-containing chromatin and the centromeric components could be confirmed by double staining with aPMM, aP3 and ACA or aCENP-A antibodies (Fig. 3C, left), or with aPMM, aP3 and atubulin antibodies that stained the kinetochore microtubules (Fig. 3C, right). However, despite the extensive overlap, the PMM and H3T3phos, and the ACA and aCENP-A signals were always distinct from each other (Fig. 3C, magnified images), suggesting that these modifications occur primarily in the inner centromeric zone (an area distinct from the inner kinetochore plate and the outer centromeric region that contains CENP-A). This interpretation is in full agreement with the biochemical observations presented in Fig. 1.

Another characteristic configuration of PMM and H3T3phos was detected soon after the cells entered anaphase. In contrast to what one might have expected from the pattern observed in metaphase, early anaphase cells exhibited little or no centromeric staining. Instead, strong PMM and H3T3phos signals were detected in the distal part of segregating chromatids, yielding a fleeing 'fingertip'

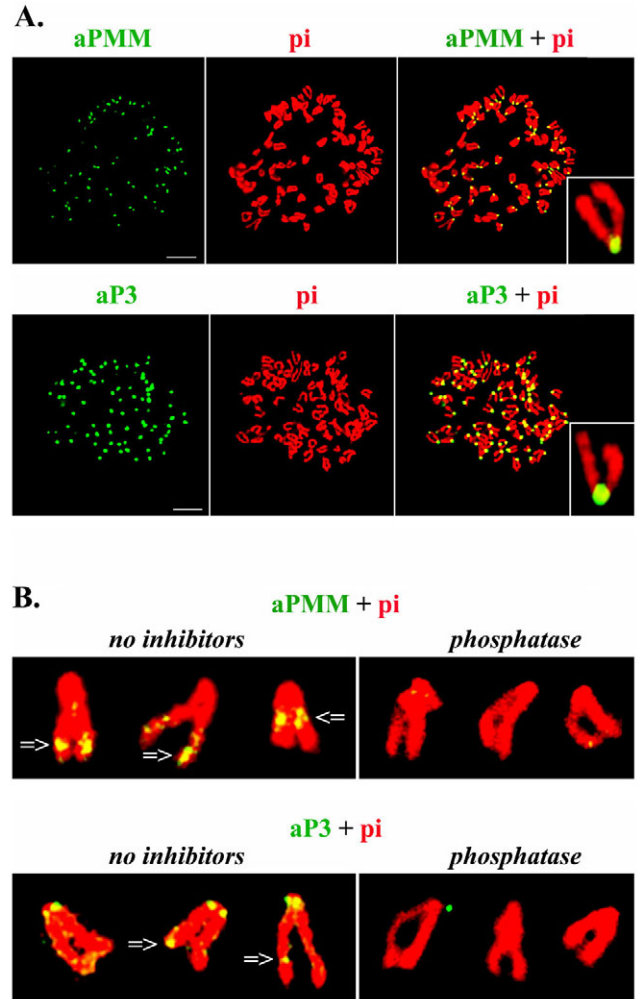


**Fig. 4.** De-localization of PMM and H3T3phos upon partial dephosphorylation. (A) Panoramic profiles of unfixed chromosome spreads decorated with aPMM and anti-P3 under phosphorylating conditions. Separate channels plus merges are shown in all cases. The insets in the lower right depict magnified profiles of individual chromosomes. Scale bars: 5  $\mu$ m. (B) Selected examples of chromosomes from spreads prepared in the absence of phosphatase inhibitors (no inhibitors) or after treatment with alkaline phosphatase (phosphatase). Arrows indicate PMM and H3T3phos foci that have apparently moved along the chromatid axis as they became partially dephosphorylated.

pattern that disappeared in telophase (Fig. 3A, early anaphase, telophase). This pattern was apparently missed in previous morphological studies investigating H3T3phos localization during mitosis (Polioudaki et al., 2004; Dai et al., 2005).

Similar results were obtained when we examined a variety of mitotic cells of human, mouse and plant (onion) origin. As a rule, early G1 cells, or cells that had entered a G0 state were not decorated beyond background levels by the anti PMM and aP3 antibodies (data not shown).

#### Distribution of PMM sites in chromosome spreads and chromatin fibers

To examine in more detail the metaphase pattern of PMM and H3T3phos and prove that the focusing around centromeres does not arise from fixation artefacts, we examined unfixed spreads of metaphase chromosomes. In agreement with our previous

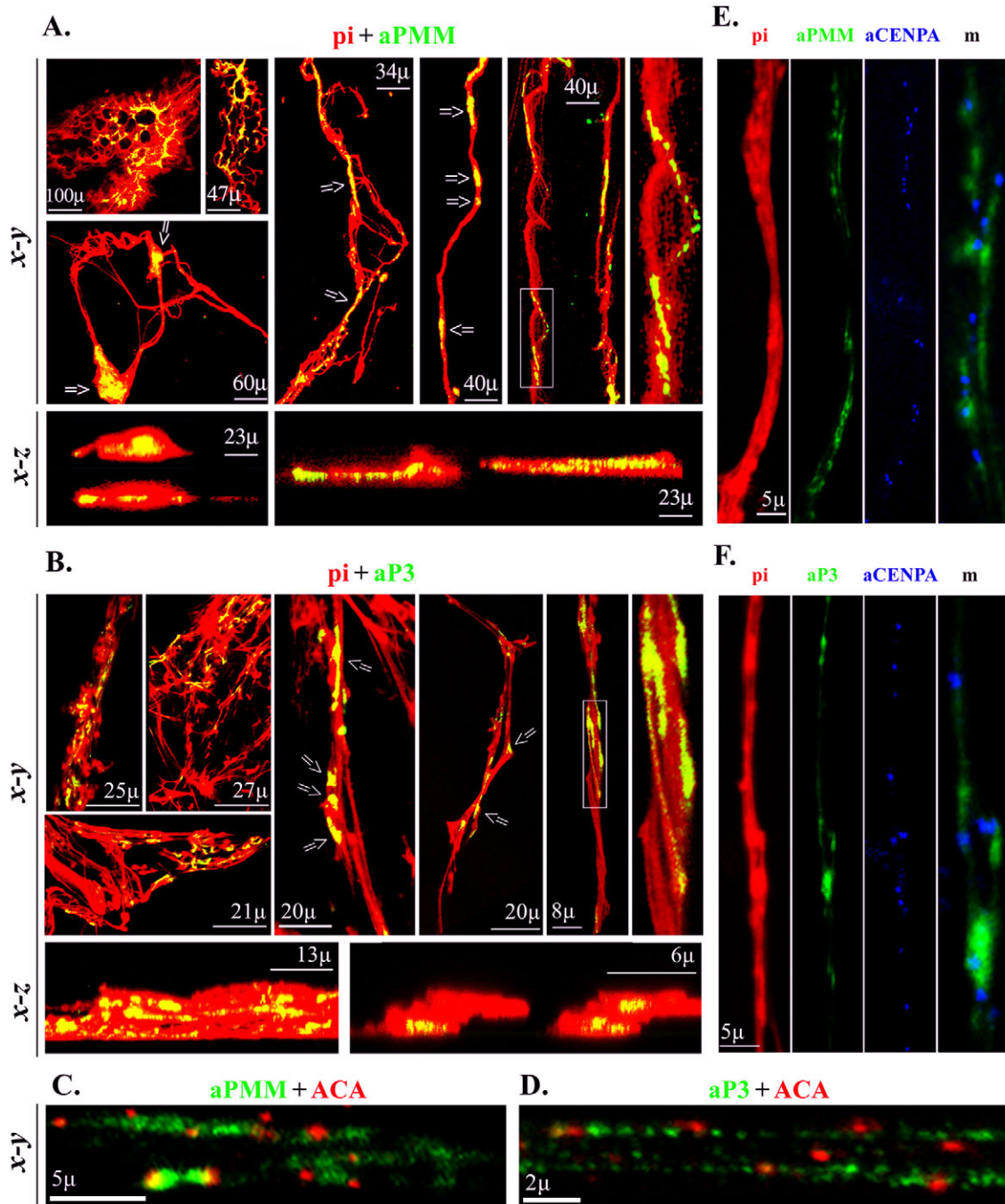


**Fig. 5.** Distribution of PMM and H3Tphos sites in unraveled chromosomes and extended chromatin fibers. Staining of partially unraveled metaphase chromosomes and extended chromatin fibers by aPMM (A) or aP3 (B) antibodies and counter-staining with propidium iodide (pi). Selected *x-y* and *x-z* sections are shown. Arrows in A and B indicate areas of periodic immunostaining. (C) Staining of chromatin fibers with aPMM (C) or aP3 (D) and ACA. (E) Triple staining of chromatin fibers with aPMM (E) or aP3 (F), aCENP-A and propidium iodide. Separate panels are shown together with a magnified merged image (m). Magnification in each panel is as specified by the bars.

observations, focal staining was observed in the centromeric area of all chromosomes (Fig. 4A) and the aPMM and aP3 signal disappeared completely when the preparations were treated with exogenous phosphatase (Fig. 4B, phosphatase). However, we also noticed that when staining of the spreads was done under conditions allowing partial dephosphorylation (i.e. in the absence of phosphatase inhibitors), the centromeric foci of PMM and H3T3phos were smaller or completely absent, with intense

fluorescence appearing now in the distal segments of the chromatids (Fig. 4B, no inhibitors). Under these conditions, the chromosome staining pattern was strikingly similar to the pattern seen in intact mitotic cells during early anaphase (compare magnified images of Fig. 4B to the anaphase patterns shown in Fig. 3A). This suggested that the apparent translocation of PMM-marked chromatin from centric to distal chromosomal sites is due to a structural alteration induced by dephosphorylation.

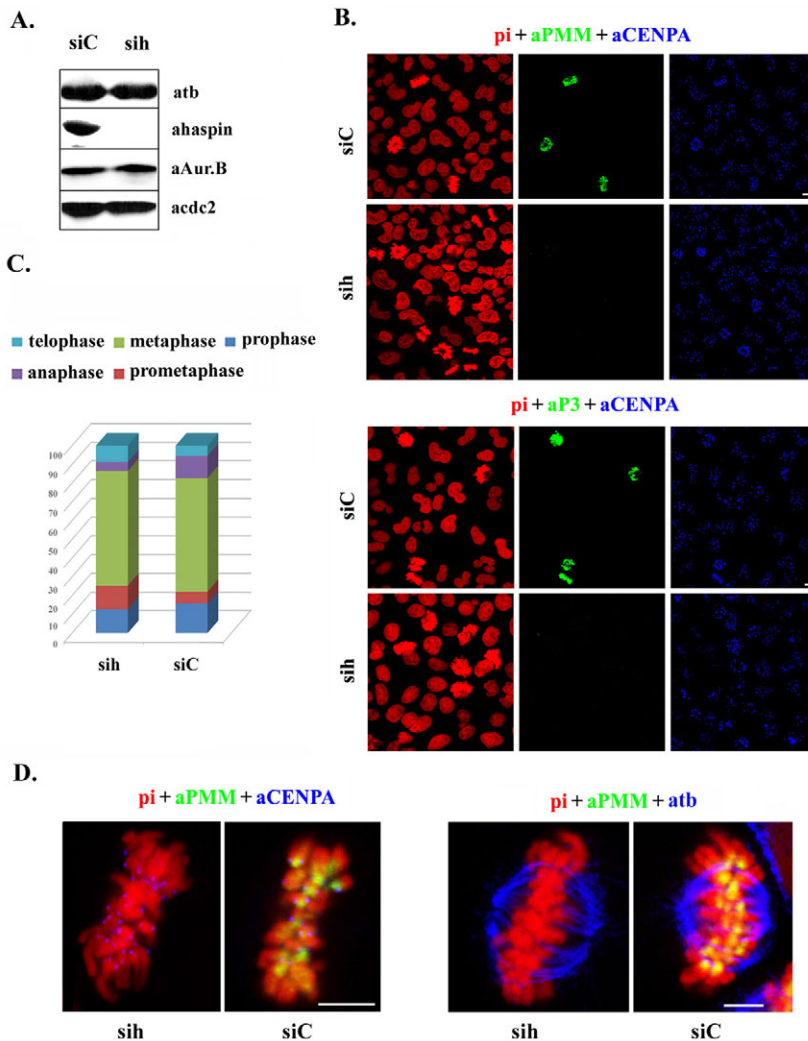


**Fig. 6.** Effects of haspin knockdown. (A) Haspin, Aurora B and cdc-2 expression in control, and in cells treated with scrambled RNA (siC) and haspin siRNA (sih) detected by western blotting. A tubulin control is included to verify equal loading. Note that haspin expression is abolished, whereas the levels of other mitotic kinases are unaffected by the RNA interference experiment. (B) Broad field views of the control (siC) and haspin-siRNA-treated (sih) cultures after staining with propidium iodide, aPMM or aP3 and aCENP-A. Note the absence of PMM or H3T3phos in all mitotic cells appearing in the haspin siRNA specimens. (C) Distribution of mitotic figures in the various phases of mitosis in control (siC) and haspin-siRNA-treated (sih) specimens. Note the relative increase of prometaphase and the corresponding decrease in the anaphase-telophase cells in the second case. (D) Detail of control (siC) and haspin-siRNA-treated (sih) mitotic cells after staining with aPMM and either aCENP-A or anti-tubulin antibodies. Note the normal appearance of centromeric foci that contain CENP-A, the metaphase plate and the spindle microtubules. Scale bars: 5  $\mu$ m.

With that in mind, we examined the organization of PMM-marked chromatin in moderately unravelled chromosomes or extended chromatin fibers that had been stretched by a factor of 10-100, depending on the conditions (see Materials and Methods). When partially unfolded metaphase chromosomes were stained with aPMM, the modified sites were still detected in groups, creating the impression of a honeycomb structure (Fig. 5A, upper left panels). However, upon further unfolding, a discontinuous, quasi-regular, pattern became apparent, revealing a series of PMM islets that were separated by longer segments of unmodified chromatin (Fig. 5A, upper middle and right panels). Viewing the specimens along the  $x$ - $z$  axis, we discovered that the PMM sites were located in the core of the chromatin fibers, indicating a certain degree of internal organization (Fig. 5A, lower panels). Similar patterns were obtained when we used aP3 antibodies (Fig. 5B).

Assessment of the relative distribution of PMM-marked and CENP-containing chromatin along the same fiber confirmed the close spatial relationship between the two chromatin domains (Fig. 5C-F). In fact, areas exhibiting an alternating ACA and aCENP-A, and aPMM and aP3 pattern, probably arising from the collapse of a looped domain that contains repeating CENP, and PMM and H3T3phos subdomains, were evident in these specimens. This result is most consistent with what has been previously observed with CID and H3S10phos in extended fibers prepared from *Drosophila*

chromatin (Blower et al., 2002). A more detailed interpretation of the chromosome spread and chromatin fiber data is provided in the Discussion.

#### Establishment of the H3T3phos mark and the PMM signature in vivo

Knowing that PMM-marked chromatin is dynamically rearranged during mitosis, we sought to determine how this signature forms and how much is influenced by the cellular context. As mentioned earlier, previous studies had suggested that H3T3phos is catalyzed by the kinase haspin (Dai et al., 2005), but it was not entirely clear whether this enzyme is essential for establishing the combinatorial modification PMM and whether this has any impact on chromosome structure. To answer these questions, we performed a series of siRNA experiments using three haspin-specific oligonucleotides and one scrambled RNA control. As shown in Fig. 6A, the siRNAs suppressed the expression of haspin without affecting other mitotic kinases, such as cdc-2 and Aurora B. At the same time, Haspin suppression decreased the staining of mitotic cells by aP3 and aPMM to background levels (Fig. 6B). From these results, we concluded that haspin is essential for the introduction of the H3T3phos mark and the formation of the PMM signature in vivo.

Cells deprived of haspin and lacking H3T3phos- and PMM-modified chromatin were delayed in exiting mitosis, as could be

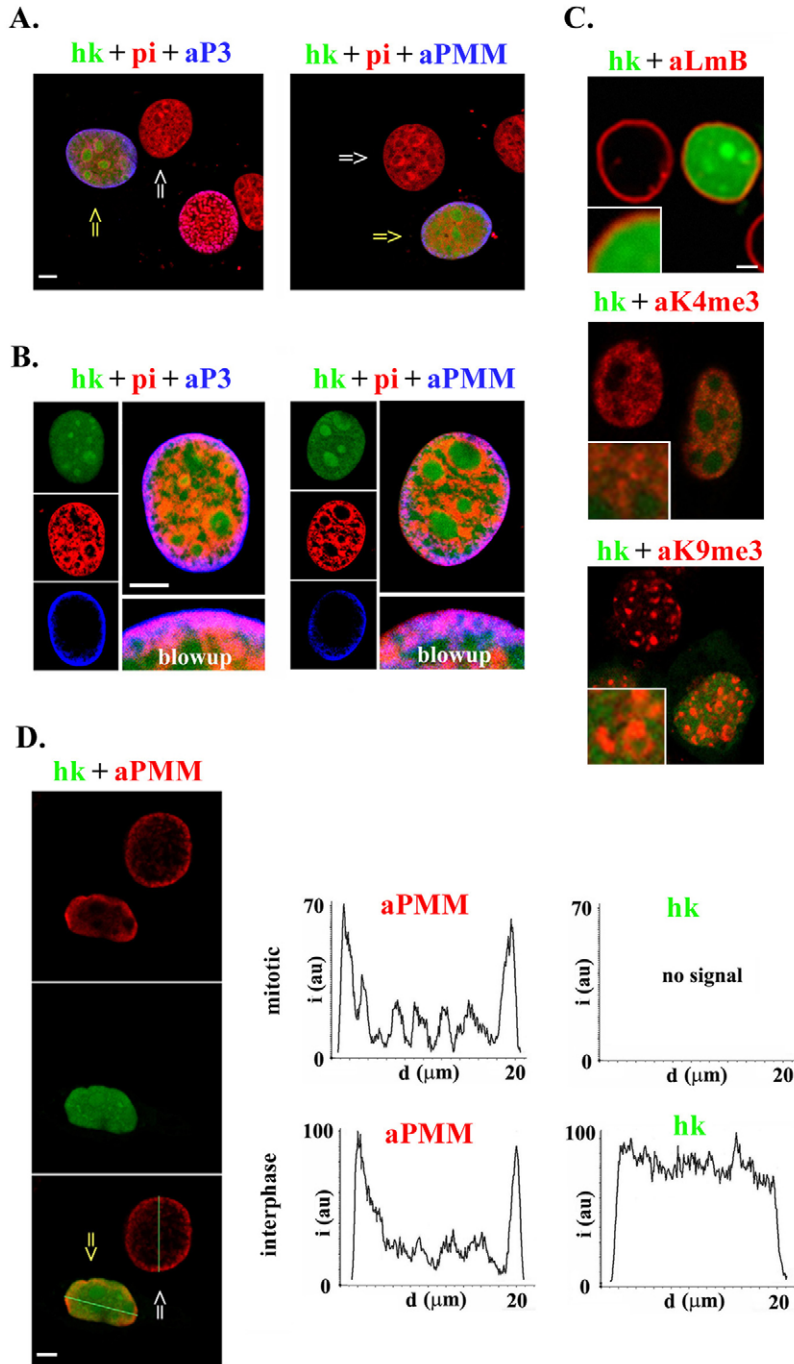


**Fig. 7.** Introduction of the H3T3phos and PMM modifications in haspin-transfected cells. (A) Survey of unsynchronous cultures transfected with EGFP-haspin (hk) and stained with aP3 or aPMM antibodies. White arrows indicate non-transfected cells and yellow arrows haspin-transfected cells. Note that only transfected cells are stained with aP3 and aPMM antibodies. (B) Profiles of interphase cells transfected with EGFP-haspin and stained with aPMM or aP3 in more detail. Separate channels plus merges and highly magnified profiles of selected regions (blowup) are shown in all cases. Note that peripheral chromatin is more heavily modified. (C) Profiles of transfected and non-transfected cells decorated with alamin B, aH3K4me<sub>3</sub>, and aH3K9me<sub>3</sub> antibodies. Insets show parts of transfected cells in greater detail, indicating that the nuclear lamina and the regions containing euchromatin or heterochromatin markers are not affected by ectopic haspin expression. (D) A typical field containing a non-transfected prophase cell (white arrow) and a neighboring haspin-transfected interphase cell (yellow arrow) stained with aPMM. The panel on the left depicts separate channels and merge. Quantitative data comparing the fluorescence intensities in the red and the green channels are presented on the right. Note that the PMM signals are of comparable intensity and are detected primarily at the periphery of the cell nucleus. Scale bars: 5 μm.

inferred from the almost twofold increase in the relative percentages of prometaphase figures and the corresponding decrease of anaphase-telophase cells in comparison with the control (Fig. 6C). The mitotic index in all siRNA-treated samples was also slightly higher (~11% difference in four independent experiments) when compared with the samples that had received scrambled RNA.

In general, the cell cycle differences observed between haspin-expressing and haspin-deficient cells were in reasonable agreement with the results published previously (Dai et al., 2005). However, a thorough morphological scrutiny of the specimens showed that haspin-deficient, PMM-negative cells did not exhibit significant chromosomal abnormalities or mis-alignment (Fig. 6D, left), spindle

defects (Fig. 6D, right), and changes in the epigenetic landscape (data not shown). We discuss this seemingly contradictory result later.

Another issue that we found worth pursuing was whether PMM formation is a primary mitotic event, or requires a specific chromatin state that develops after the cells pass the G2-M checkpoint. To address this problem, we induced ectopic formation of H3T3phos by overexpressing the haspin kinase in cultured cells. In these experiments, we used a minimal construct, containing the C-terminal kinase domain of the enzyme, which is constitutively active and does not need to be mitotically activated as does the full-length protein (Y.M. and S.D.G., unpublished observations). Inspecting asynchronous cultures, we observed that cells expressing EGFP-

haspin, both interphase and mitotic, were always aP3 and aPMM positive, whereas interphase cells that did not express the enzyme were negative with both antibodies (Fig. 7A). From this, we concluded that introduction of H3T3phos and formation of the PMM mark do not require a pre-existing mitotic state.

Upon closer inspection, we also noticed that H3T3phos and PMM islands developing in interphase chromatin after ectopic expression of haspin were much more prominent at the periphery of the cell nucleus, a fact that was highly reminiscent of that previously observed in naturally occurring prophase cells (Fig. 7B; compare with Fig. 3A). The preferential modification of peripherally located chromatin was not due to trapping of the enzyme by the nuclear lamina or insufficient release from the nuclear pore complex. As shown in all panels of Fig. 7, EGFP-haspin was efficiently imported into the nucleus (presumably through an intrinsic NLS located between residues 391-394) and filled the entire nucleoplasm. Nucleoli were often penetrated as the enzyme accumulated in the nucleus (the same has been observed when full-length haspin or other nuclear proteins are expressed in cultured cells) (see Dai et al., 2005), but there was no indication for selective retention in regions of peripheral heterochromatin. Gross alterations of peripheral sub-structures, apoptotic phenomena and global chromatin rearrangements potentially triggered by overexpression of haspin could also be ruled out by staining the transfected cells with a battery of antibodies recognizing the nuclear lamins and several different histone modifications, such as H3K9me<sub>3</sub>, H3K4me<sub>3</sub> etc. (Fig. 7C; and data not shown).

The selective modification of peripheral chromatin could be confirmed by measuring the fluorescence intensity across the nucleus in transfected interphase cells and in non-transfected mitotic cells (Fig. 7D). Furthermore, from quantitative morphometric data, it could be seen that the degree of modification by ectopically expressed haspin during interphase was comparable with that occurring normally in prophase (same intensity of aPMM staining under the same conditions). Taking this into account, and inspecting a large number of cells stained with DNA dyes more closely (Fig. 7A-B, panels pi), we confirmed that premature formation of H3T3phos and PMM domains does not affect chromatin condensation. This supports the fact that haspin-deficient cells lacking the H3T3phos and PMM mark possess normally condensed chromosomes and do not exhibit apparent defects in the area of the kinetochore. Therefore, although the formation of PMM is a founding mitotic event, this modification does not suffice on its own for initiating a mitotic chromatin state.

## Discussion

### Occurrence of the PMM mark and organization of PMM-marked chromatin

Using chromatin immunoprecipitation and mass spectrometry, we identified PMM, a new combinatorial modification in the N-terminal tail of histone H3. This combinatorial mark consists of H3T3phos, H3K4me<sub>3</sub> and H3R8me<sub>2</sub>, and occurs specifically in mitosis, as confirmed by staining cells with aPMM antibodies. PMM is detected initially at peripheral sites of the prophase nucleus and then in the centromeric area of condensed chromosomes. However, the apparent association with the centromere does not imply coincidence: in metaphase cells the PMM signal and the ACA and CENP-A signals are distinct, whereas in early anaphase cells, the spatial proximity of PMM to centromeric determinants ceases to exist.

The dynamic transitions of PMM-marked chromatin can be better understood by comparing the PMM distribution patterns in intact

metaphase plates, chromosome spreads and extended chromatin fibers. From such studies, it becomes clear that PMM-marked chromatin organizes as compact, centromere-associated domains when metaphase chromosomes are folded and as interspersed islets when the chromosomes are split or unraveled and the chromatin components partially dephosphorylated.

The grouping and scrambling of PMM sites along the chromatin fiber can be explained by a reversible association among non-contiguous PMM subdomains depending on the degree of histone H3 phosphorylation. The idea that H3 phosphorylation modulates the lateral binding of PMM subdomains is based on several structural studies. Specifically, Arya and Schlick (Arya and Schlick, 2006) have shown that charge neutralization of the histone H3 tails, which is expected to occur when a multiplicity of phosphate groups are added next to lysine and arginine residues, dissociates the extended H3 tails from the linker DNA and confers ability for internucleosomal hydrogen bonding. This greater hydrogen bonding regime has also been detected when we used molecular dynamics to investigate the potential interactions between modified and non-modified histone tails (G. Papamokos, S.D.G. and A.S.P., unpublished) and is consistent with a recently published report that investigated the effect of histone H3 phosphorylation on local chromatin state using a bona fide structural approach (Eberlin et al., 2008).

### Potential functions of PMM

What could be the biological meaning of the intricate, ever-changing patterns of PMM observed during mitosis? This question impinges on a still unresolved issue, originally discussed and investigated in relation to histone H3 phosphorylation at Ser10 (H3S10phos). H3S10phos has been proposed to function in different ways, affecting chromosome compaction through preferential polyamine binding (Sauve et al., 1999) or selective recruitment of condensation factors (Wei et al., 1999; Cheung et al., 2000). In addition to these scenarios, which are equally probable for PMM, Higgins and coworkers have recently shown that H3T3phos, the modification catalyzed by haspin, co-distributes with cohesin and could potentially mediate sister chromatid association (Dai et al., 2006).

As attractive as they might be, all these scenarios have weak points. For instance, despite the fact that H3T3phos co-distributes with cohesin, direct binding of H3T3phos peptides to this protein does not seem to occur (Dai et al., 2006). Second, although chromosome condensation generally coincides with histone H3 phosphorylation during mitosis, topoisomerase II and SMC proteins bind with identical, very low affinity to both native and tailless nucleosomes (de la Barre et al., 2000; Kimura and Hirano, 2000). And, finally, although a simplified experimental system does not account for the potential contribution of other proteins and histone modifications that are present in cells (Dai et al., 2006), it should be taken into account that normal-looking chromosomes can be assembled in *Xenopus* extracts without the need for histone H3 phosphorylation (MacCallum et al., 2002; Prigent and Dimitrov, 2003).

There is no doubt that the patterns of PMM-marked chromatin observed during mitosis have something to do with chromatin fiber packing and centromere organization. In that respect, it would be reasonable to propose that the PMM mark contributes to the better presentation of the kinetochore area to the microtubules, facilitating the formation of an asymmetric hub with the CENP-A regions on its external face and the modified histone H3 regions in its inner core (see above). However, there are three points that need to be considered when we correlate this mark with chromosome structure.

First, as indicated by mass spectrometry data, PMM does not exist in isolation, and is embedded into a more complex modification platform that probably affects how it operates *in vivo*. Second, apart from histone H3 modifications that affect PMM in *cis*, it is likely that folded chromatin imposes other constraints that act in *trans* to this mark, creating 'collective' properties that emerge only at the level of the entire chromosome system (Laughlin, 2005).

Taking these points into account, and considering the results of haspin knockdown and haspin overexpression reported here, we feel more akin to the idea originally proposed by Hans and Dimitrov: that PMM, similarly to H3S10phos, might organize a transient structural motif along the chromosome surface that serves as a 'ready' production label or as 'licensing system' that distinguishes chromosomes that have successfully passed through the metaphase-anaphase checkpoint (Hans and Dimitrov, 2001). This would explain why elimination of PMM affects exit from mitosis without causing gross chromosomal defects and why ectopic formation of this combinatorial signature, although highly reminiscent of early prophase events, does not trigger the mitotic cycle by itself.

## Materials and Methods

### Cell lines and antibodies

Both (human) HeLa cells and (mouse) C-127 cells were used. Cells were grown in Dulbecco's modified Eagle's medium (DMEM), supplemented with 10% FBS, 1% penicillin-streptomycin and 1% L-glutamine at 37°C and 5% CO<sub>2</sub>. Synchronization at M phase was achieved by treating the cells with 80 ng/ml nocodazole for 18 hours. The following antibodies were used: aP3 (Polioudaki et al., 2004) and aPMM or aK4me<sub>3</sub>-R8me<sub>2</sub> in their affinity-purified form; ACA (kindly provided by Haralampos M. Moutsopoulos, University of Athens School of Medicine, Athens, Greece); aH3K9me<sub>3</sub> and aH3S10phos (obtained through Prim B. Singh, Borstel Institute, Liebniz, Germany); ap34/cdc2, aSNF2, aH3K9ac, aH3K27me<sub>3</sub>, aH3K4me<sub>2</sub> and aH3K4me<sub>3</sub> (purchased from Upstate); aCENP-A and aHaspin (purchased from Abcam); aAurora B and  $\alpha$ -tubulin (purchased from Sigma). HP1 $\alpha$  was identified by a polyclonal rabbit antiserum (M235), affinity-purified over the recombinant protein. Anti-desmin and anti-lamin-B antibodies were prepared and purified in house. Anti-histone modification antibodies (aP3 and aPMM) were raised in rabbits. Affinity purification of these antibodies was done as follows. Immune sera (diluted 1:15 in PBS or undiluted) were incubated with an equal volume of peptide-Sulfolink (Pierce) at a peptide concentration of 1 mg/ml for 2 hours at room temperature. The column was washed with five volumes of high salt buffer (250 mM NaCl, 10 mM Tris-HCl pH 7.4, 1 mM EGTA) and then 10 volumes of isotonic salt buffer (150 mM NaCl, 10 mM Tris-HCl pH 7.4, 1 mM EGTA). Elution of specifically bound immunoglobulin was done with 100 mM glycine-HCl pH 2.3, 1 mM EGTA and 150 mM NaCl. Fractions of 0.5 ml were collected and immediately neutralized with 40  $\mu$ l of 1 M Tris base at 0°C. The fractions were analyzed by SDS-PAGE, pooled, adjusted to 0.2% Triton X-100 and 0.1% fish skin gelatin and dialyzed overnight at 4°C against isotonic salt buffer. Affinity purified antibodies were cross-absorbed against recombinant (non-modified) histone H3, as needed. This histone form was purified from bacterial lysates according to published methods (Agalioti et al., 2002).

### Constructs and transfection

A C-terminal segment of the haspin kinase [residues 391-798 (Dai et al., 2005)] was amplified from HeLa cell cDNA. The primers used were: forward, 5'-CCGCTCGAGGCACAAGAAGAAAATTGTGACT-3'; reverse, 5'-CCGGAATTCTTACTTAAACAGACTGTGCTGGCA-3'. The resulting PCR product was subcloned into pEGFP-C2 vector. Transfection was carried out by effectene (Qiagen), according to manufacturer's instructions, or by electroporation using the ECM630 apparatus (BTX) operated at 200-260 V, 850  $\mu$ F, 725  $\Omega$ . Cells were fixed 12-24 hours after transfection.

### RNA interference

Human haspin validated siRNAs (ID: 1093, 141030, 242467) and scrambled RNA (ID# AM4642) were purchased from Ambion and used at 20 nM to transfect HeLa cells. Transfection was carried out with Lipofectamine RNAiMAX reagent obtained from Invitrogen and the cells were analyzed after 48-72 hours.

### Microscopy

Cells grown on coverslips were washed, fixed in 1-4% formaldehyde in phosphate-buffered saline, permeabilized with 0.2% Triton X-100 and blocked with 0.5% fish skin gelatin. The specimens were visualized in a Leica SP confocal microscope.

### Cytological preparations

Chromosome spreads were prepared as described (Jeppesen, 1994) with the following modifications: KCM buffer included 1 mM PMSF, 50 mM NaF, 0.1  $\mu$ M okadaic acid, 20 mM  $\beta$ -glycerol phosphate and protease inhibitors. Dephosphorylation of the preparation was accomplished by a 30 minute treatment with 10 U/ $\mu$ l of shrimp alkaline phosphatase before antibody incubation.

### Preparation of chromatin fibers

Extended chromatin fibers were prepared from synchronized mitotic cells (see below), using a variation of the method described (Sullivan and Karpen, 2004). Specifically, synchronized mitotic cells were resuspended in 75 mM KCl, 10 mM HEPES-KOH pH 7.4, 1.5 mM MgCl<sub>2</sub>, 50 mM NaF, 20 mM  $\beta$ -glycerol phosphate, 1 mM PMSF and protease inhibitors at a final concentration of  $3.5 \times 10^4$  cells/ml. A sample of 400  $\mu$ l of the cell suspension was spun in a ShandonCytospin 4 centrifuge for 5 minutes at 1000 g onto a coated slide. The slide was incubated for 15 minutes in lysis buffer (25 mM Tris-HCl pH 7.5, 0.5 M NaCl, 0.2% Triton X-100, 0.5 M urea), washed twice with PBS for 2 minutes and fixed in 4% formaldehyde in PBS for 20 minutes. The specimens were examined by indirect immunofluorescence as described above. Chromonemata (i.e. bundles consisting of many chromatin fibers) and partially relaxed chromosomes were prepared in a similar manner, omitting urea from the buffer.

### Cell fractionation and chromatin immunoprecipitation

Nocodazole-arrested HeLa or C-127 cells were collected by shake-off. Mitotic cells were resuspended in KHM buffer (78 mM KCl, 50 mM HEPES-KOH, pH 7.4, 4 mM MgCl<sub>2</sub>, 8.37 mM CaCl<sub>2</sub>, 10 mM EGTA, 1 mM DTT, 1 mM PMSF, 1 mM ATP, 20  $\mu$ M cytochalasin D, 3  $\mu$ M Microcystin-LR, 20 mM  $\beta$ -glycerol phosphate, 20 mM phosphocreatine, 400  $\mu$ g/ml creatine kinase and protease inhibitors used at standard concentrations) and Dounce homogenized. Mitotic chromosomes collected after centrifugation were digested twice with DNase I (50  $\mu$ g/ml, 15 minutes at room temperature). After controlled sonication (four times for 5 seconds at 40 W) a crude chromatin fraction was collected by low-speed centrifugation. Finally, the residue after DNaseI digestion was extracted with EDTA and the particles released in the three supernatants were combined and adjusted in 0.3 M NaCl, 1% Triton X-100. The supernatant after ultracentrifugation at 100,000 g was used for chromatin immunoprecipitation. Chromatin immunoprecipitations were carried out by overnight incubation with antibodies at 0°C, followed by incubation for 1 hour with Protein G beads. Beads were blocked in 1% fish skin gelatin before use. Precipitates were washed five times with 150 mM NaCl, 10 mM PIPES pH 7.0, 1 mM EGTA, 1% Triton X-100, 0.1% fish skin gelatin and once with the same buffer without Triton X-100 and fish skin gelatin. Samples were analyzed by SDS-PAGE.

### Mass spectrometry

Matrix-assisted laser desorption ionization time-of-flight mass spectrometry (MALDI-TOF) was performed at the Functional Genomics Unit of Moredun Research Institute (Edinburgh, UK). Protein bands were digested with arginine-specific protease. Peak assignment was done either manually or using Applied Biosystems programs.

### ELISA and western blotting

Enzyme-linked immunosorbent assays (ELISA) were performed as described (Polioudaki et al., 2004). Western blotting and analysis in sucrose density gradients were performed according to standard procedures.

This work was supported by the programs Herakleitos and Pythagoras II from the Hellenic Ministry of Education and by the program PENED 2003 from the General Secretariat for Research and Technology, Ministry of Development, which are co-funded by EU-ESF and National sources. Y.M. was supported in part by a graduate fellowship from FORTH/BRI. We thank George Papamokos (University of Ioannina, Greece) for providing unpublished information, E. Kaxiras (Harvard University) for providing computational facilities and Carol Murphy (FORTH/BRI) for advice on siRNA experiments. The paper is dedicated to Lazaros Apekis.

## References

- Agalioti, T., Chen, G. and Thanos, D. (2002). Deciphering the transcriptional histone acetylation code for a human gene. *Cell* **111**, 381-392.
- Arya, G. and Schlick, T. (2006). Role of histone tails in chromatin folding revealed by a mesoscopic oligonucleosome model. *Proc. Natl. Acad. Sci. USA* **103**, 16236-16241.
- Berstein, B. E., Mikkelsen, T. S., Xie, X., Kamal, M., Huebert, D. J., Cuff, J., Fry, B., Meissner, A., Wernig, M., Plath, K., Jaenisch, R., Wagschal, A., Feil, R., Schreiber, S. L. and Lander, E. S. (2006). A bivalent chromatin structure marks key developmental genes in embryonic stem cells. *Cell* **125**, 315-326.
- Blower, M. D. and Karpen, G. H. (2001). The role of Drosophila CID in kinetochore formation, cell-cycle progression and heterochromatin interactions. *Nat. Cell Biol.* **3**, 730-739.

- Blower, M. D., Sullivan, B. A. and Karpen, G. H.** (2002). Conserved organization of centromeric chromatin in flies and humans. *Dev. Cell* **2**, 319-330.
- Cheung, P., Allis, C. D. and Sassone-Corsi, P.** (2000). Signaling to chromatin through histone modifications. *Cell* **103**, 263-271.
- Crowe, S. L., Movsesyan, V. A., Jorgensen, T. J. and Kondratyev, A.** (2006). Rapid phosphorylation of histone H2A.X following ionotropic glutamate receptor activation. *Eur. J. Neurosci.* **23**, 2351-2361.
- Dai, J., Sultan, S., Taylor, S. S. and Higgins, J. M.** (2005). The kinase haspin is required for mitotic histone H3 Thr 3 phosphorylation and normal metaphase chromosome alignment. *Genes Dev.* **19**, 472-488.
- Dai, J., Sullivan, B. A. and Higgins, J. M.** (2006). Regulation of mitotic chromosome cohesion by Haspin and Aurora B. *Dev. Cell* **11**, 741-750.
- de la Barre, A. E., Gerson, V., Gout, S., Creaven, M., Allis, C. D. and Dimitrov, S.** (2000). Core histone N-termini play an essential role in mitotic chromosome condensation. *EMBO J.* **19**, 379-391.
- De Souza, C. P., Osmani, A. H., Wu, L. P., Spotts, J. L. and Osmani, S. A.** (2000). Mitotic histone H3 phosphorylation by the NIMA kinase in *Aspergillus nidulans*. *Cell* **102**, 293-302.
- Eberlin, A., Grauffel, C., Oulad-Abdelghani, M., Robert, F., Torres-Padilla, M. E., Lambrot, R., Spehner, D., Ponce-Perez, L., Wurtz, J. M., Stote, R. H. et al.** (2008). Histone H3 tails containing dimethylated lysine and adjacent phosphorylated serine modifications adopt a specific conformation during mitosis and meiosis. *Mol. Cell. Biol.* **28**, 1739-1754.
- Fischle, W., Tseng, B. S., Dormann, H. L., Ueberheide, B. M., Garcia, B. A., Shabanowitz, J., Hunt, D. F., Funabiki, H. and Allis, C. D.** (2005). Regulation of HPI-chromatin binding by histone H3 methylation and phosphorylation. *Nature* **438**, 1116-1122.
- Georgatos, S. D., Pyrpassoulou, A. and Theodoropoulos, P. A.** (1997). Nuclear envelope breakdown in mammalian cells involves stepwise lamina disassembly and microtubule-drive deformation of the nuclear membrane. *J. Cell Sci.* **110**, 2129-2140.
- Hake, S. B., Garcia, B. A., Kauer, M., Baker, S. P., Shabanowitz, J., Hunt, D. F. and Allis, C. D.** (2005). Serine 31 phosphorylation of histone variant H3.3 is specific to regions bordering centromeres in metaphase chromosomes. *Proc. Natl. Acad. Sci. USA* **102**, 6344-6349.
- Hans, F. and Dimitrov, S.** (2001). Histone H3 phosphorylation and cell division. *Oncogene* **20**, 3021-3027.
- Hendzel, M. J., Wei, Y., Mancini, M. A., Van Hooser, A., Ranalli, T., Brinkley, B. R., Bazett-Jones, D. P. and Allis, C. D.** (1997). Mitosis-specific phosphorylation of histone H3 initiates primarily within pericentromeric heterochromatin during G2 and spreads in an ordered fashion coincident with mitotic chromosome condensation. *Chromosoma* **106**, 348-360.
- Jeppesen, P.** (1994). Immunofluorescence techniques applied to mitotic chromosome preparations. *Methods Mol. Biol.* **29**, 253-285.
- Jiang, L., Smith, J. N., Anderson, S. L., Ma, P., Mizzen, C. A. and Kelleher, N. L.** (2007). Global assessment of combinatorial post-translational modification of core histones in yeast using contemporary mass spectrometry: LYS4 trimethylation correlates with degree of acetylation on the same H3 tail. *J. Biol. Chem.* **282**, 27923-27934.
- Kimura, K. and Hirano, T.** (2000). Dual roles of the 11S regulatory subcomplex in condensin functions. *Proc. Natl. Acad. Sci. USA* **97**, 11972-11977.
- Laughlin, R. B.** (2005). *A Different Universe: Reinventing Physics From The Bottom Down*. New York: Basic Books.
- MacCallum, D. E., Losada, A., Kobayashi, R. and Hirano, T.** (2002). ISWI remodeling complexes in *Xenopus* egg extracts: identification as major chromosomal components that are regulated by INCENP-aurora B. *Mol. Biol. Cell* **13**, 25-39.
- Phanstiel, D., Brumbaugh, J., Berggren, W. T., Conard, K., Feng, X., Levenstein, M. E., McAlister, G. C., Thomson, J. A. and Coon, J. J.** (2008). Mass spectrometry identifies and quantifies 74 unique histone H4 isoforms in differentiating human embryonic stem cells. *Proc. Natl. Acad. Sci. USA* **105**, 4093-4098.
- Polioudaki, H., Markaki, Y., Kourmouli, N., Dialynas, G., Theodoropoulos, P. A., Singh, P. B. and Georgatos, S. D.** (2004). Mitotic phosphorylation of histone H3 at threonine 3. *FEBS Lett.* **560**, 39-44.
- Preuss, U., Landsberg, G. and Scheidtmann, K. H.** (2003). Novel mitosis specific phosphorylation of histone H3 at Thr11 mediated by Dlk/ZIP kinase. *Nucleic Acids Res.* **31**, 878-885.
- Prigent, C. and Dimitrov, S.** (2003). Phosphorylation of serine 10 in histone H3, what for? *J. Cell Sci.* **116**, 3677-3685.
- Rogakou, E. P., Pilch, D. R., Orr, A. H., Ivanova, V. S. and Bonner, W. M.** (1998). DNA double-stranded breaks induce histone H2AX phosphorylation on serine 139. *J. Biol. Chem.* **273**, 5858-5868.
- Sauve, D. M., Anderson, H. J., Ray, J. M., James, W. M. and Roberge, M.** (1999). Phosphorylation-induced rearrangement of the histone H3 NH2-terminal domain during mitotic chromosome condensation. *J. Cell Biol.* **145**, 225-235.
- Shoemaker, C. B. and Chalkley, R.** (1978). An H3 histone-specific kinase isolated from bovine thymus chromatin. *J. Biol. Chem.* **253**, 5802-5807.
- Sullivan, B. A. and Karpen, G. H.** (2004). Centromeric chromatin exhibits a histone modification pattern that is distinct from both euchromatin and heterochromatin. *Nat. Struct. Mol. Biol.* **11**, 1076-1083.
- Taverna, S. D., Ilin, S., Rogers, R. S., Tanny, J. C., Lavender, H., Li, H., Baker, L., Boyle, J., Blair, L. P., Chait, B. T. et al.** (2006). Yng1 PHD finger binding to H3 trimethylated at K4 promotes NuA3 HAT activity at K14 of H3 and transcription at a subset of targeted ORFs. *Mol. Cell* **24**, 785-796.
- Trojer, P. and Reinberg, D.** (2008). A gateway to study protein lysine methylation. *Nat. Chem. Biol.* **4**, 332-334.
- Wei, Y., Yu, L., Bowen, J., Gorovsky, M. A. and Allis, C. D.** (1999). Phosphorylation of histone H3 is required for proper chromosome condensation and segregation. *Cell* **97**, 99-109.